CRYSTAL GROWTH & DESIGN

pubs.acs.org/crystal

Article

Supramolecular Isomerism in Cobalt(II) Coordination Polymers Built from 3,5-Bis(trifluoromethyl)benzoate and 4,4′-Bipyridine

Francesco Papi, Albert Rosado, Oriol Vallcorba, Arianna E. Lanza, Mauro Gemmi,* Núria Portolés-Gil, Ana M. López-Periago, Concepción Domingo, and José A. Ayllón*

Cite This: *Cryst. Growth Des.* 2022, 22, 4463−4471

Read Online

ACCESS | Metrics & More | Article Recommendations | Supporting Information

ABSTRACT: The reaction of $[Co_2(H_2O)(TFMBz)_4(py)_4]$ (**1**) (TFMBz: 3,5-bis(trifluoromethyl)benzoate; py: pyridine) with 4,4′-bipyridine (bpy) in different solvents yields four coordination polymers with unlikely structures but with the same stoichiometry. Three of them contain similar ladder chains consisting of binuclear nodes "$Co_2(TFMBz)_4$", in which two of the TFMBz ligands show bidentate bridge coordination, double linked to each adjacent node by bpy but packed in different fashions. The different packing affects the compound porosity; thus, $[Co_2(TFMBz)_4(bpy)_2]_n$ (**2**), precipitated using low-polarity solvents such as supercritical CO_2 ($scCO_2$), *n*-butyl acetate, or heptane and also in acetonitrile, is microporous, with a surface area of 330 $m^2\ g^{-1}$, showing the N_2 adsorption/desorption isotherm at 77 K with a gate-opening effect at low relative pressures (P/P_0 = 0.05). The isomer $[Co_2(TFMBz)_4(bpy)_2]_n$ (**3**), synthesized in ethoxyethanol, presents a surface area of 230 $m^2\ g^{-1}$. A third chain packing isomer, $[Co_2(TFMBz)_4(bpy)_2]_n$ (**4**), is obtained in acetone and has only non-interconnected voids. Finally, precursor **1** is combined with bpy in a highly polar solvent such as water to give $[Co(TFMBz)_2(bpy)]_n$ (**5**). In this isomer, all the carboxylate units act as bidentate bridging ligands, generating chains that are interlinked by bpy, leading to a 2D network, which after packing yields a non-porous structure. The resolution of structures **2**−**5** is only possible with the recently developed 3D electron diffraction method based on the collection of diffraction patterns on sub-micron-sized single crystals. The variation of magnetic susceptibility as a function of temperature is also measured. Overall, our work provides insightful information on the complex landscape of metal−organic framework solids that are formed by crystallization using different solvent media.

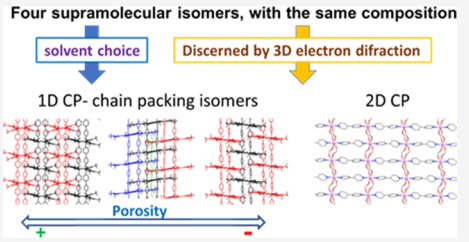

INTRODUCTION

Research in metal−organic frameworks (MOFs) and coordination polymers (CPs) is a continuously advancing area of development. Much effort has been devoted to the design and controlled crystallization of these coordination networks, shaped with transition metal atoms and multifunctional bridging ligands, owing to their potential key applications in adsorption, separation, heterogeneous catalysis, and so forth.[1−5] The phenomenon of polymorphism, for example, the ability of a crystalline material to adopt different crystal structures, is of paramount importance to determine the chemical and physical properties of the material.[6] The concept of polymorphism, clearly established in the pharmaceutical industry for molecular compounds, was extended to oligomeric and polymeric coordination compounds by Zaworotko *et al.*, defining supramolecular isomerism as the existence of more than one superstructure for a given set of components.[7,8] Supramolecular isomerism is of particular importance in CPs since the superstructure plays an essential role in determining the properties of these crystalline materials. This concept is challenging, but it is crucial for fundamental understanding to speed up the development of CP-based functional materials.[9]

Concepts of reticular chemistry are exploited to generate application-driven MOFs, with a structure that, in principle, can be anticipated from the used set of precursor entities, including metal centers, counter anions, and linkers. However, often this is not the situation because of the poor understanding of the role played by different experimental parameters in the growth of a defined CP. Moreover, the packing in a 1D or 2D network is still more difficult to anticipate due to the subtle attractive or repulsive force that prevails in the crystal lattice. The preparation of MOF isomers is serendipitous in nature; thus, achieving controlled synthesis of supramolecular isomers remains a long-term challenge.[10] The tendency of some MOFs to polymorphism has been related to the low energy differences between the lattice energy for diverse polymorphs of only a few kcal mol^{-1}.[6] Experimental factors, such as the temperature, reagent concentration, pH, solvent, presence of additional species in the medium (additives, template/guests), crystallization method, and so forth, would determine the particular isomer obtained in a

Received: April 7, 2022
Revised: May 19, 2022
Published: June 2, 2022

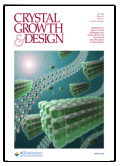

https://doi.org/10.1021/acs.cgd.2c00406
Cryst. Growth Des. 2022, 22, 4463−4471

designed synthetic process.[9,11] Among all these factors, the use of different solvents to precipitate different supramolecular isomers is relatively common.[11−13] Different solvent properties may favor the formation of distinct isomers: polarity, ability of solvent molecules to coordinate with the metal ion, binding to the crystal nucleus, formation of loose aggregates of several solvent molecules that can serve as effective templates, and so forth. Thus, varying the energy barrier leads to different polymorphs.[14,15]

The number of polymorphs identified from a specific combination of metal nodes and ligands is generally related to the number of different experimental conditions assayed, although frequently scientists focused the scientific study on a given polymorph rather than on the search and characterization of possible alternative isomers. Moreover, polymorphs that present some difficulties to be obtained as single crystals are prone to be discarded. Thus, the importance of polymorphism in MOFs and CPs is under-represented in the scientific literature and should be more widely investigated.

Supramolecular isomerism is usually referred to CPs with a framework that contains the same nodes and linkers in the same ratio but differ in the nature or number of solvent molecules incorporated to the framework, thus presenting different crystal structures. This concept implies small differences in the composition and, strictly speaking, should be defined as pseudo-polymorphism.[16−18] Examples of supramolecular isomerism in CPs, with a fixed stoichiometry for the framework constituents and pending or occluded solvents, are scarce.[19,20] Pure isomerism in MOFs and CPs is an area particularly interesting from a scientific point of view. Indeed, elimination of the differences in the composition (solvent) of the polymorphic materials would help in the analysis of the structure−property relationship.[21] There are many reports in the literature describing the synthesis of two isomers, while only few have given details of three pure isomers.[19,22] In this work, we give one of the first examples of a system with four different isomers, which were crystallized from a new dinuclear cobalt(II) benzoate having trifluoromethyl substituents in positions 3 and 5 (TFMBz). This metal node was reacted with 4,4′-bipyridine (bpy), one of the most studied ditopic linkers in CPs (Scheme 1).[23] Although both the metal ligand TFMBz and the linker bpy are mostly rigid molecules with only a limited rotational degree of freedom, the results of this work show how the solvent used in precipitation determines the precise supramolecular isomer that is formed. Advanced techniques for crystal structure elucidation, namely, single-crystal diffraction analysis using synchrotron radiation and 3D electron diffraction (3D ED), were needed to describe the precipitated compounds. The use of these techniques plays a key role in correctly assessing the structural and physical differences between the isomers even with the characterization of isomers of different dimensionality. The description of the overall results aims to demonstrate the general under-rated importance of structural isomerism in molecular crystal engineering and provide a basis for understanding and rationalizing supramolecular isomorphism in MOFs and CPs.

Scheme 1. Structure of the bpy Linker and the TFMBz Ligand with Three Different Coordination Modes for Co^{II} Found in Compounds 1−5: Bidentate Bridging Coordination Mode (μ^2:η^1,η^1), Monodentate, and Chelation, Respectively

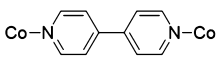

4,4′-bipyridine

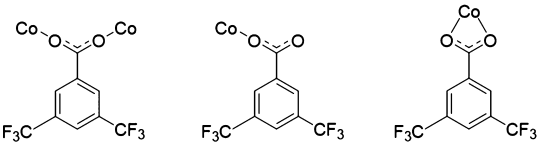

3,5-bis(trifluoromethyl)benzoate

EXPERIMENTAL SECTION

Materials. $Co(CH_3COO)_2{\cdot}4H_2O$, 3,5-bis(trifluoromethyl)benzoic acid (HTFMBz), pyridine (py) and 4,4′-bipyridine (bpy) and all the solvents (acetonitrile, ethoxyethanol, heptane, acetone, and *n*-butylacetate) were purchased from Sigma-Aldrich and used without further purification. Ultrapure water (Milli-Q system, conductivity lower than 0.05 $\mu S\ cm^{-1}$) was used. Compressed CO_2 (99.95%) was supplied by Carburos Metálicos S.A.

Synthesis of Compounds 1−5. *Synthesis of $[Co_2(H_2O)(TFMBz)_4(py)_4]$ (**1**).* HTFMBz (1.555 g, 6.02 mmol) and $Co(CH_3COO)_2{\cdot}4H_2O$ were dissolved in methanol (100 mL), and the resulting fuchsia solution was evaporated on a hot plate at 65 °C, giving a highly viscous oil. This product was heated on a ventilated furnace at 100 °C for 1 h to eliminate possible traces of the acetic acid by-product. The final residue was dissolved in ethanol (100 mL) together with 1.0 mL (12.7 mmol) of pyridine. Then, 25.0 mL of water was added. The resulting pink solution was allowed to slowly evaporate at room temperature, and a crystalline solid, which appears after partial evaporation of the ethanol, was filtered and washed repeatedly with water and, finally, dried on air. The yield was about 90 wt %. Anal. Calcd for $C_{56}H_{34}O_9N_4F_{24}Co_2$ (1480.7 g mol^{-1}): C, 45.42; H, 2.31; N, 3.78. Found: C, 45.54; H, 2.14; N, 3.74%.

*Synthesis of $[Co_2(TFMBz)_4(bpy)_2]_n$ (**2**).* This compound can be obtained in supercritical CO_2 ($scCO_2$) or in conventional organic solvents, such as acetonitrile, *n*-butylacetate, or heptane.

Route A. Reactions in $scCO_2$ were performed in a 5 mL Pyrex vial placed into a 100 mL high pressure autoclave with two opposite sapphire windows (TharDesign). The vial was charged with 200 mg of compound **1** (0.135 mmol) and 50 mg (0.320 mmol) bpy. A small magnetic stirrer was also added, and the vial was finally capped with cellulose filter paper. Experiments were performed at 20 MPa and 60 °C. The vial was stirred at 500 rpm. After a running period of 20 h, the product was washed with fresh $scCO_2$ to eliminate any excess of bpy ligand, free pyridine by-product, and other possible residues. The autoclave was then depressurized and cooled down to room temperature to recover a green powder. Yield *ca.* 70 wt %. Anal. Calcd for $C_{56}H_{28}O_8N_4F_{24}Co_2$ (1458.7 g mol^{-1}): C, 46.11; H, 1.93; N, 3.84. Found: C, 46.32; H, 2.07; N, 3.69%.

Route B. The same product previously obtained in $scCO_2$ was precipitated by dissolution of the same precursors in the same ratio in several conventional solvents, specifically heptane, acetonitrile, or *n*-butylacetate. In the case of heptane, it was necessary to use boiling solvent to favor the solubility of precursor **1**, and also, it was the choice for acetonitrile to favor crystallinity. For the three solvents, the recovered precipitates were washed twice with the same solvent (hot) to eliminate residual reagents.

*Synthesis of $[Co_2(TFMBz)_4(bpy)_2]_n$ (**3**).* A solution of compound **1** (120 mg, 0.081 mmol) in ethoxyethanol at 50 °C was mixed with a solution of bpy (26.0 mg, 0.167 mmol) in the same solvent and temperature. After mixing, a crystalline precipitate was obtained with a yield of *ca.* 62 wt %. Anal. Calcd for $C_{56}H_{28}O_8N_4F_{24}Co_2$ (1458.7 g mol^{-1}): C, 46.11; H, 1.93; N, 3.84. Found: C, 45.87; H, 2.03; N, 3.60%.

*Synthesis of $[Co_2(TFMBz)_4(bpy)_2]_n$ (**4**).* A solution of compound **1** (120 mg, 0.081 mmol) in acetone at room temperature was mixed

https://doi.org/10.1021/acs.cgd.2c00406
Cryst. Growth Des. 2022, 22, 4463−4471

with a solution of bpy (26.0 mg, 0.167 mmol) in the same solvent and temperature. After mixing, a crystalline precipitate was obtained in a yield of *ca.* 83 wt %. Anal. Calcd for $C_{56}H_{28}O_8N_4F_{24}Co_2$ (1458.7 g mol^{-1}): C, 46.11; H, 1.93; N, 3.84. Found: C, 46.12; H, 1.80; N, 3.66%.

Synthesis of $[Co(TFMBz)_2(bpy)]_n$ (**5**). 209 mg of compound **1** (0.141 mmol) was dissolved in 100 mL of boiling water, and then a solution of 45 mg (0.288 mmol) of bpy in hot water was added under vigorous agitation, leading to the precipitation of a pink solid. The heating and stirring were maintained for 30 min. Then, the solid was filtered, washed with hot water, and dried in air. Yield *ca.* 91 wt %. Anal. Calcd for $C_{56}H_{28}O_8N_4F_{24}Co_2$ (1458.7 g mol^{-1}): C, 46.11; H, 1.93; N, 3.84. Found: C, 46.31; H, 1.92; N, 3.65%.

Detailed procedures for the characterization of the materials are included in the Supporting Information.

RESULTS AND DISCUSSION

Synthesis and Characterization. A binuclear cobalt $[Co_2(H_2O)(TFMBz)_4(py)_4]$ (**1**), including benzoate ligands with two trifluoromethyl groups and pyridine that could be obtained in as a pure crystalline material in high yields was chosen as a node precursor for the synthesis of CPs. This pyridine adduct has the advantage of being soluble in a wide variety of solvents, from heptane to water, as well as in supercritical CO_2. While compound **1** is partially soluble in many solvents of intermediate polarity at room temperature, heating of the solvent to boiling or near-boiling temperature is necessary to achieve a significant dissolution in either polar water or nonpolar heptane.

Initial trials showed that very different results are obtained as a function of the solvent choice, leading, in some cases, to mixtures of compounds. Powder XRD characterization allows to determine some solvents that allow to precipitate four different compounds, even if elemental analysis (C, H, and N) suggested that all of them have the same stoichiometry, $[Co(TFMBz)_2(bpy)]$. Crystal structure elucidation confirmed these findings. Hence, $[Co_2(TFMBz)_4(bpy)_2]_n$ (**2**) was obtained in $scCO_2$, heptane, *n*-butylacetate, or acetonitrile, while the remaining three isomers were obtained in ethoxyethanol, $[Co_2(TFMBz)_4(bpy)_2]_n$ (**3**), acetone, $[Co_2(TFMBz)_4(bpy)_2]_n$ (**4**), and water, $[Co(TFMBz)_2(bpy)]_n$ (**5**).

A priori, it is expected for all the isomers that the bpy linker displaces the four pyridine ligands present in **1** during the reaction, thus leading to a 3D framework if the orientation of bpy preserves the original orientation of the initial pyridine ligands. Actually, 3D-MOFs in which subunits of a dinuclear Co^{II} carboxylate with an aqua bridge are connected by the bpy linker[24] or by other ditopic *N,N*-bipyridine ligands[25,26] have been reported. However, in all the essayed experimental conditions of this work, the aqua bridge present in **1** was lost during the pyridine substitution reaction by bpy to produce different CPs, independently of the solvent used.

Interestingly, ATR-FTIR spectra reflected variations in the coordination mode of the TFMBz ligand of the four isomers. Hence, significant differences were observed in the region corresponding to the $\nu_{as}(COO^-)$ band, in the 1650−1550 cm^{-1} ranges and also in the 850−700 cm^{-1} fingerprint region (Figure S1). In these regions, **2**, **3**, and **4** show a similar pattern between them, while **5** shows a different one. This could be explained after crystal structure elucidation, which established that in isomer **5**, all TFMBz ligands show the bidentate bridging coordination mode (μ^2:η^1,η^1), while in the other three isomers (**2**−**4**), only half of the TFMBz ligands display this type of coordination and the other half shows the chelating coordination mode (Scheme 1).

Crystal Structures. *Crystal Structure of* $[Co_2(H_2O)(TFMBz)_4(py)_4]$ (**1**). Compound **1** belongs to the triclinic crystal system, with the space group $P\bar{1}$ (**2**). The asymmetric unit contains two Co^{II} atoms, four TFMBz, four pyridine, and one aqua ligand. In each binuclear molecule, the two Co^{II} are held together through two syn,syn μ^2:η^1,η^1-carboxylate bridges from TFMBz ligands and one bridging aqua ligand, as shown in Figure 1. The distorted octahedral geometry around each

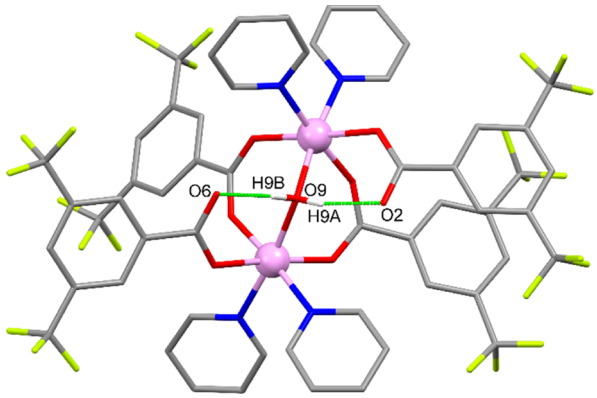

Figure 1. Crystal structure of compound **1**. Color code: C gray; O red; N blue, Co pink, and F green. Hydrogen atoms, except those of the aqua ligand (in white), are omitted for clarity. Hydrogen bond between the aqua and the carboxylate ligands are depicted as dotted green lines.

metal ion is completed by one oxygen from an additional monodentate TFMBz ligand and two nitrogen donor atoms from two pyridine ligands, leading to a local $[(N_{py})_2(O_{TFMBz})_3(O_{water})]$ coordination sphere around each metal center. The hydrogen atoms of the aqua bridge are involved in intramolecular O(9)−H···O−C hydrogen bond, with the uncoordinated O atom of the monodentate TFMBz ligand (Table 1). The O_{water}−H distance was about 2 times

Table 1. H Bond Interactions in Compound 1[a]

D−H···A	D−H	H···A	D···A	D−H···A
O(9)−H(9A)···O(2)	0.86(3)	1.81(3)	2.613(1)	155(3)
O(9)−H(9B)···O(6)	0.85(3)	1.72(3)	2.540(2)	164(3)

[a]Hydrogen-bond geometry (Å, deg).

lower than the H···O_{TFMBz} distance, confirming that the bridging O atom belongs to water. The two Co−O(9) bond length distances of 2.145(1) and 2.157(1) Å, the Co(1)−O(9)−Co(2) angle of 116.87(5),° and the Co−N_{py} bond lengths in the range 2.138−2.176 Å are comparable to those reported for other aqua bridged binuclear Co^{II} carboxylates.[27−30]

Crystal Structures of Compounds **2**, **3**, *and* **4**. The reaction between compound **1** and 4,4′-bipyridine in the mentioned solvents (different from water) yielded, after displacement of the pyridine and aqua ligand of the precursor, three pure isomers containing all similar 1D ladder type chains. Compound **2** can be prepared in $scCO_2$, heptane, *n*-butylacetate, or acetonitrile; compound **3** is obtained in ethoxyethanol; and compound **4** precipitates in acetone. In the three cases, roughly planar binuclear "$Co_2(TFMBz)_4$" nodes

https://doi.org/10.1021/acs.cgd.2c00406
Cryst. Growth Des. 2022, 22, 4463−4471

are observed, where the two Co^{II} ions are double bridged by carboxylate groups of two of the TFMBz ligands, while each of the two additional TFMBz ligands coordinates to one Co^{II} through a chelating carboxylate (Figures 2 and S2). Four

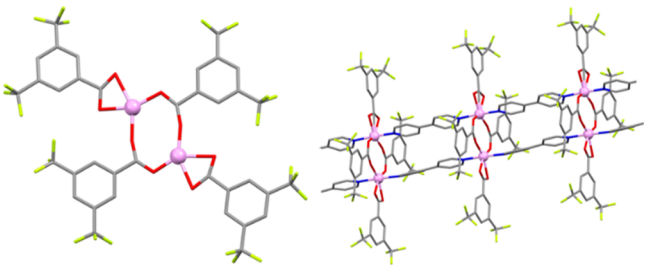

Figure 2. Binuclear $Co_2(TFMBz)_4$ SBUs and ladder chains observed in the crystal structure of compound **3**. Color code: C gray; O red; N blue, Co pink, and F green. H atoms are omitted. H atoms are omitted.

bipyridine linkers connect each binuclear subunit with its nearest neighbors in opposite directions, forming ladder chains of approximately 11.6 Å step and leading to a 1D CP (Figures 2 and S2). Ladder chains containing carboxylate ligands and Co^{II} and bpy linkers, similar to those found in compounds **2**–**4**, have previously been described.[31−33] The almost planar binuclear "$Co_2(TFMBz)_4$" motif can be regarded as a secondary building unit (SBU) similar to some reported molecular compounds that contain analogous binuclear clusters bonded to four monodentate pyridines.[34−36]

The most fascinating aspect of the crystal structures of compounds **2**–**4** is their different crystal packing despite being formed by similar ladder chains. In Figure 3, the crystal structures of the three compounds are viewed along the chains, to envisage the differences in the packing. Each binuclear subunit projects four TFMBz ligands roughly perpendicular to the chain axis in different directions. The relative arrangement of these TFMBz ligands determines how ligands belonging to close neighbor chains interact and therefore the crystal packing.

In compound **2**, each chain, with the propagation direction parallel to the crystallographic *a* axis, has two neighbors in the *c* direction and two in the *b* direction (Figure 3a). The interchain interaction is stronger with the nearest neighbor, found in the *c* direction, in which the protruding TFMBz ligand interdigitate clearly. Contrarily, when the nearest neighbor is in the perpendicular direction (*c* axis), the interpenetration is much less pronounced (Figure S3). Besides, alternated orientations of the binuclear SBU are observed when looking along the *c* direction (Figure S3). Isomer **3** also shows a chain propagation direction parallel to the crystallographic *a* axis but a different packing in which the intertwined chains give rise to supramolecular layers parallel to the *ab* plane (Figure 3b). In this case, a tighter interdigitation is observed since in the void between two "$Co_2(TFMBz)_4$" of each chain, protruding TFMBz of two other neighbor chains, interdigitate (instead of only one as observed for **2**), thus favoring weak $\pi-\pi$ stacking interactions (Cg···Cg 3.85 Å) (Figure S4). Finally, compound **4** shows another different packing of chains (Figure 3c). In this case, the interdigitation between close neighbors due to the protruding TFMBz, lies roughly in middle position between two successive "$Co_2(TFMBz)_4$" SBU in a chain, as it was also observed for **2** (Figure S5). The nearest neighbor in a

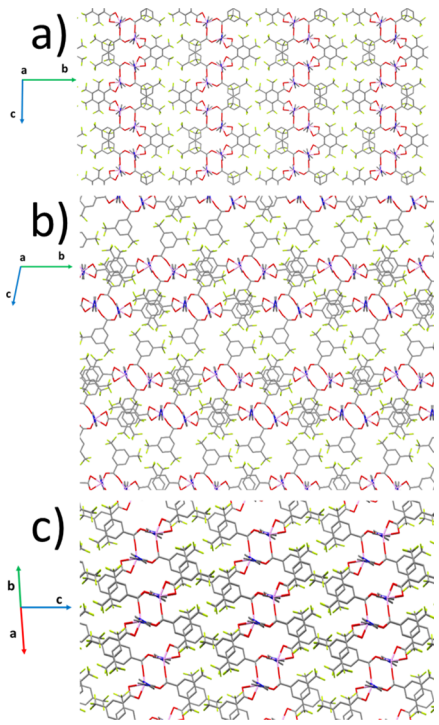

Figure 3. Different packing of the ladder chains in the crystal structures of compounds **2** (a), **3** (b), and **4** (c). **2** contains disordered bpy and TFMBz ligands, not shown for clarity. Color code: C gray; O red; N blue, Co pink, and F green. H atoms are omitted.

perpendicular direction shows negligible interpenetration, although the position of the "$Co_2(TFMBz)_4$" SBU in the chain axis direction shifts steadily (Figure S5). Besides the $\pi-\pi$ stacking interactions observed in **3**, the three alternative packings favor inter-chain contacts that are established through the trifluoromethyl groups of the TFMBz ligand (F···F contacts) and through the hydrogen atom of the bpy ligand (F···H−C contacts). Interestingly, compounds **2**, **3**, and **4** are porous materials albeit to a different extent. Void analysis using Mercury software shows that the accessible space gives rise to a crystal channel in isomer **2** (22.2% of unit cell volume, 1645 $Å^3$) and in isomer **3** (15.1%, 465 $Å^3$), while **4** (6.5%, 101 $Å^3$) only contains non-interconnected voids (Figure S6).

Crystal Structure of Compound ***5****.* When the reaction between compound **1** and bpy is carried out in water, the totally different product **5** is obtained. In **5**, all TFMBz carboxylate groups show the bidentate bridge coordination mode, leading to the formation of chains (Figure 4a) instead of the discrete binuclear subunits found in the former compounds. In these chains, in which Co^{II} ions are separated by about 5.0 Å, the four coordinating oxygens define a plane. To complete the approximately octahedral coordination of Co^{II}, the two axial positions, perpendicular to this O_4 plane, are occupied by nitrogens from bpy linkers. Consequently, chains are connected by the bpy linkers, ultimately defining a 2D CP (Figure 4b). Structure analysis reveals a compact packing of layers with weak intermolecular contacts, namely, dispersive forces established between trifluoromethyl groups from adjacent layers (Figure 4c). In **5**, however, the formation of the bridged chain of Co^{II} ions over the planar "$Co_2(TFMBz)_4$" SBU sterically prevents TFMBz ligands to interact by $\pi-\pi$ stacking, in favor of a tight assembly of layers resulting in a

https://doi.org/10.1021/acs.cgd.2c00406
Cryst. Growth Des. 2022, 22, 4463−4471

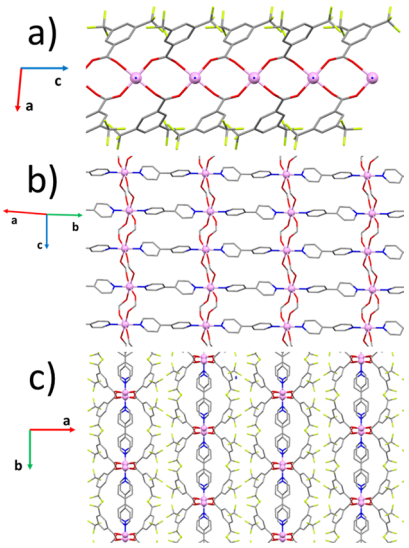

Figure 4. Crystal structure of compound **5**. (a) Chains of Co^{II} ions, separated by about 5.0 Å, generated, thanks to the bridging bidentate TFMBz ligands. (b) Completion of the coordination sphere of the Co^{II} by N atoms from ditopic bpy linkers gives rise to a 2D framework. (c) Structure analysis reveals a compact packing of layers, with weak intermolecular contacts through trifluoromethyl groups. Color code: C gray; O red; N blue, Co pink, and F green. H atoms are omitted. In (b), only the carboxylate group of each TFMBz ligand is shown for clarity.

non-porous compound. Only one structure has been found based on chains of Co^{II} supported by bridging carboxylates and interconnected by bpy, defined as a 2D framework.[37] Moreover, although Co^{II} species of different nuclearity (dimers, trimers, tetramers, *etc.*)[38] based on carboxylate bridges have been described, only one compound in which these bridges extend into a 1D polymer has been previously reported.[39] In this compound, the coordination of Co^{II} is completed by monodentate pyridines, so the overall structure is 1D. Interestingly, all these compounds have been prepared hydrothermally, hence suggesting that water favors the formation of bridging carboxylates.

Polymorphism and Solvent Effect. As mentioned previously, polymorphism based on the different packing of identical substructures is rare.[40] Only a few examples of CPs that present crystal structures differentiated basically by the packing mode of similar chains have been described. A clear example found in the literature is the two crystalline polymorphs of compound catena-(μ^2-2,5-dimethylpyrazine-*N*,*N*′)-dibromido-zinc(II) that contain topologically identical chains packed in a different fashion.[41] Furthermore, for the closely related compounds $\{[Mn_3(hpdc)_2(H_2O)_6]_3{\cdot}2H_2O\}_n$ and $\{[Mn_3(hpdc)_2(H_2O)_6]_3{\cdot}H_2O\}$ (H_3hpdc = 2-hydroxypyrimidine-4,6-dicarboxylic acid), the two elucidated structures contain similar one-dimensional chain components but packed with different orientations, either staggered or plywood-like stacked, respectively. Both compounds differ only in the content of crystallization water.[42,43] Recently, three polymers of the type $[(Cu(hfa)_2)(3\text{-tpt})]_n$ [hfa = hexafluoroacetylacetonate, 3-tpt = 2,4,6-tris(3-pyridyl)-1,3,5-triazine] have been described, whose composition only differs in the incorporated crystallization solvent molecules but forms structures differing in dimensionality and porosity.[12] Actually, a survey of the scientific literature regarding MOF supramolecular isomerism indicates that many authors do not take into consideration differences in the content of crystallization solvents,[11] although the strict criterion to name isomerism would require exactly the same composition.[40] Overall, the crystal structures of **2**−**4** represent a major example of packing isomerism and offer interesting clues to understand how a packing mode over the others can be favored as a function of the crystallization solvent.

The crystal packing shown by compound **2** seems to be preferred in case of solvents with low polarity and low dielectric constant, notably $scCO_2$, heptane, and *n*-butylacetate. Gradually increasing solvent polarity induces the precipitation of **3**, in ethoxyethanol, and of **4**, in acetone. Interestingly, these three supramolecular isomers contain similar ladder type chains but packed in different modes. Therefore, the solvent properties strongly influence the interchain interactions and, consequently, the crystal packing observed. Acetonitrile is a particularly interesting case as it leads to the formation of **2**, despite its relatively high polarity. This suggests that additional effects are actually in play due to the differences in the interactions between the solvent and growing crystal nucleus. The use of water as a solvent determines a different behavior of the TFMBz ligand, leading to the formation of Co^{II} chains in lieu of the discrete SBU observed in the organic solvents. The combination of these chains with the bpy linker runs to the formation of a bidimensional CP. Supramolecular isomers that show different dimensionality are scarce and usually based on the use of flexible linkers.[9,13,44−48] Thus, the structures of compounds **2**−**5** are overall very interesting and allow to understand and rationalize how the solvent choice deeply affects the products obtained at a fixed stoichiometry.

Compound Pore Characteristics and Surface Area. Compounds surface area, determined by N_2 adsorption/desorption at 77 K, denote clear differences between the four supramolecular isomers: **2** (surface area of 330 $m^2\ g^{-1}$) and **3** (surface area of 230 $m^2\ g^{-1}$) are porous materials, while **4** and **5** are not. The N_2 isotherm of **2** (Figure 5) shows two distinct sections in the adsorption branch. A first noteworthy adsorption episode occurs in the region of very low relative pressure (P/P_0), the slope of the branch clearly being reduced as P/P_0 reaches the critical value of 0.05. This behavior is followed by a sudden increase in the amount of N_2 adsorbed for P/P_0 greater than 0.05, and finally, a well-defined plateau is recorded. Interestingly, the adsorption and desorption paths in the isotherm differ considerably, showing a hysteresis loop that only closes at pressures near to vacuum. This hysteresis should not be correlated with condensation in mesopores because the P/P_0 values of sudden increase and closing hysteresis are very low.[49,50] Moreover, the presence of mesopores was not found by the performed crystallographic structural determination, which highlighted only the presence of micropores. SEM characterization showed the precipitation of micrometric particles (Figure S7); therefore, the hypothesis of the generation of mesopores due to aggregation of nanoparticles was also discarded. The structural analysis indicated that the framework of **2** involves interconnected pores, although its visualization is not trivial due to ligand disorder present in the structure. Adsorption data shows that most of the pore volume was not accessible at low pressures. A plausible explanation could be that, at the low temperature of measurements, channels were initially blocked likely due to the disordered TFMBz ligands, but pressure and/or partial filling prompted

https://doi.org/10.1021/acs.cgd.2c00406
Cryst. Growth Des. 2022, 22, 4463−4471

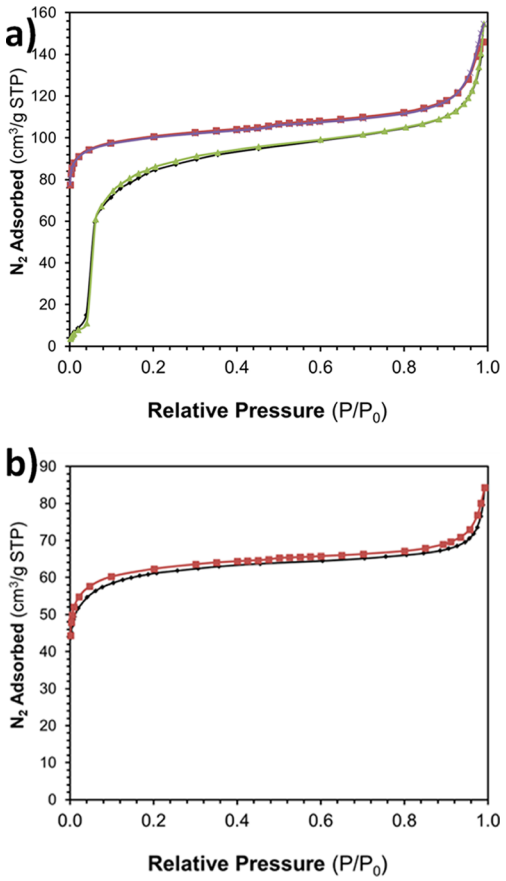

Figure 5. 77 K N_2 adsorption/desorption isotherms: (a) for compound **2**, showing two consecutive cycles; color code: 1st adsorption, black; 1st desorption red; 2nd adsorption green; 2nd desorption blue, and (b) for compound **3**.

some minor structural modifications related to increased TFMBZ ordering that makes void space available. The desorption branch indicates that very low-pressure values must be attained to empty the pores. Conversely, isomer **3** shows the common type I adsorption/desorption isotherm, suggesting that the bottleneck between voids is not an effective barrier to the diffusion of N_2; this is probably because at 77 K, the trifluoromethyl group rotation is fast enough to eliminate any impediment (Figure 5).[51,52] Finally, isomers **4** and **5** do not display a significant surface area, as expected from the presence of non-interconnected voids in **4**, resulting in non-effective porosity, and compact packing in **5**.

Magnetic Properties. The variable-temperature magnetic susceptibility of the five compounds (**1**–**5**) was measured under 1000 Oe in the temperature range 2–300 K (Figure 6). In a first approximation, $\chi_{(T)}$ data for all compounds show a good fitting to the Curie–Weiss law, $\chi_{(T)} = C/(T - \theta_{CW})$, at temperatures above 4–35 K (Table 2). The negative values of

Table 2. Fitting Parameters of the Curie–Weiss Analysis for Compounds 1–5

compound	range linearity (K)	C (emu K mol^{-1})	θ_{CW} (K)	χ_T value at 300 K (emu K mol^{-1})
1	10–300	2.95	−23.89	2.70
2	20–300	2.39	−13.79	2.27
3	20–300	2.43	−9.44	2.34
4	4–300	2.71	−12.10	2.58
5	35–300	2.72	−15.19	2.58

θ_{CW} indicate dominant antiferromagnetic exchange interactions in addition to single-ion spin–orbital coupling (Figure S8). For all compounds, the χ_T value per Co^{II} atom at 300 K is significantly larger than the spin-only value (1.87 emu K mol^{-1}) for $S = 3/2$ ions, indicative of significant contribution from the unquenched orbital momentum of Co^{II}.[53,54]

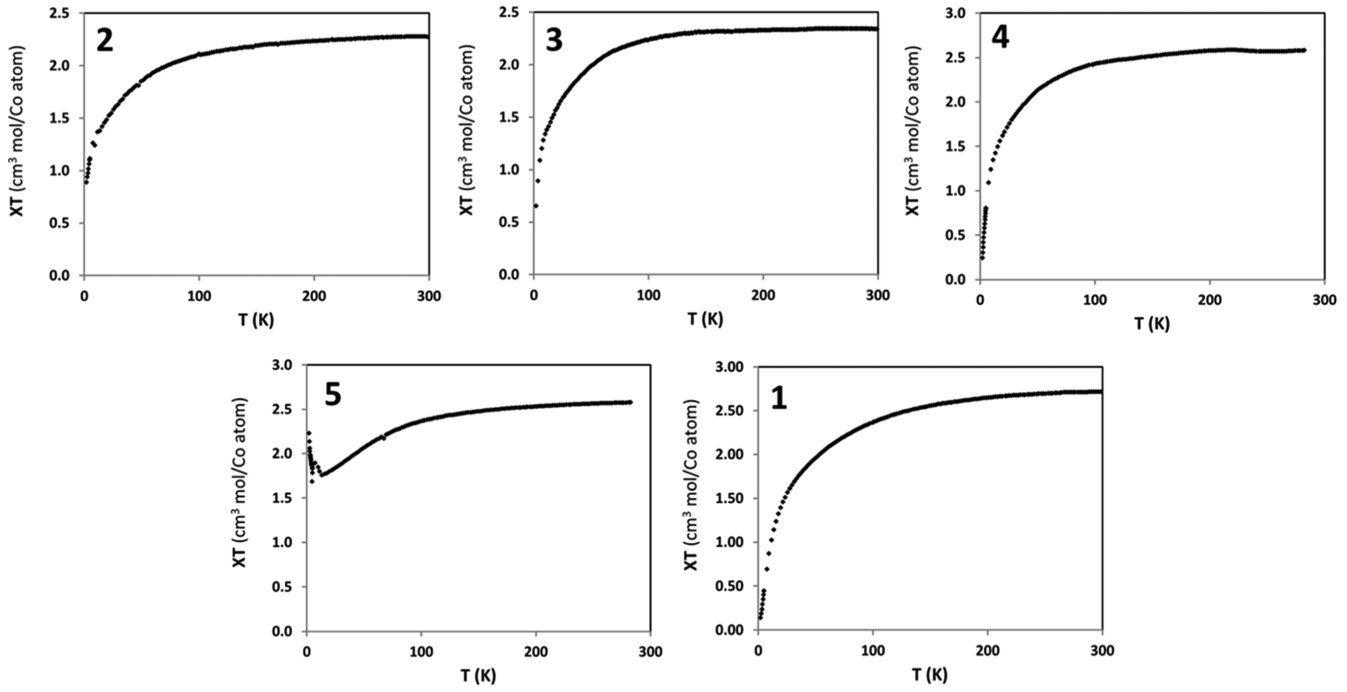

Figure 6. χ_T *vs* temperature curve for compounds **1**–**5** at an applied field of 1000 Oe.

https://doi.org/10.1021/acs.cgd.2c00406
Cryst. Growth Des. 2022, 22, 4463–4471

In **2**−**5**, the dominant exchange pathway may be established through bridging carboxylate ligands in each dimer and through the aqua bridge in compound **1**, as for all cases the $Co^{II}\cdots Co^{II}$ distances are too large to support direct through-space interaction. Despite the bpy linker connection, it is improbable that any significant interaction takes place between adjacent binuclear subunits in the chains of compounds **2**−**4**; indeed, their magnetic behavior resembles that reported for binuclear cobalt complexes.[55] Besides, the bulky nature of TFMBz prevents interactions among neighboring chains; all the $Co^{II}\cdots Co^{II}$ distances between atoms belong to different subunits being always much larger than the intradimer $Co^{II}\cdots Co^{II}$ distance. Antiferromagnetic coupling is also supported by the small χ_T values at low temperature found for compounds **1**−**4**.[53] Compound **5** presents different chains of Co^{II} centers instead of the binuclear unit but the antiferromagnetic interactions dominate above 50 K, as for the former compounds. Differences arise on cooling, when ferromagnetic interactions become more important as denoted by the variations in the χ_T values at low temperature. Magnetic characterizations of similar 2D compounds, based on interconnected Co^{II} carboxylate chains, have remarkably not been reported in the literature.

CONCLUSIONS

Supramolecular isomerism in MOFs and CPs is a major challenge in modern chemistry despite its crucial role in determining the chemical and physical properties of materials for different technological applications. Due to the limited information available in the literature, the design of supramolecular isomers still remains a complex task and the influence of a variety of experimental factors, such as solvent medium, temperature, reagents concentration, and presence of additives and guests, is not yet fully understood. The choice of solvent medium, either for synthesis or crystallization, is particularly relevant in this regard, and our results demonstrate how the properties of the solvent used actually drive the formation of different polymorphs despite the same stoichiometry. Our results have pointed out how the physical properties of the solvent employed, mostly its polarity, affect the supramolecular isomer obtained as they favor specific interchain non-covalent interactions in the frameworks formed by Co^{II}, bpy, and TFMBz. Low polarity solvents consistently lead to structures based on binuclear Co^{II} complexes, where $CF_3\cdots F_3C$ interactions from the TFMBz ligands appear to be determinant (compound **2**). Increasing the polarity of the solvent favors a different packing of the ladder chains characterized by $\pi-\pi$ stacking interactions between TFMBz ligands of adjacent binuclear Co^{II} complexes (compound **3**, obtained in ethoxyethanol). A further increase of solvent polarity, using acetone, leads to a third isomer containing similar ladder-type chains consisting of SBUs connected by bpy linkers and interacting through $CF_3\cdots F_3C$ contacts (compound **4**). However, the fact that compound **2** is obtained also in acetonitrile, a solvent with a polarity higher than acetone, shows that other properties of the solvent can likely determine which isomer precipitate. The different packing of the chains in **2**−**4** influences the porosity, as **2** and **3** show a porous nature, while **4** displays non-interconnected voids. Furthermore, water, a high polarity solvent, promotes the formation of a remarkable 2D framework defined by chains of Co^{II} ions bridged by bidentate TFMBz ligands (compound **5**). Together, these results give interesting clues about the possible design of supramolecular isomers, which could be easily extended to the supramolecular engineering of MOFs and CPs of different components and stoichiometries. It must be pointed out that the detailed study of supramolecular isomerism has been possible only because 3D ED can give structural information on sub-micrometric crystals. Without this possibility, the polycrystalline powders would have remained in the vials as unknown compounds and sooner or later would have been discarded. We can foresee that by applying this approach, many more MOFs and CPs would show a more complex phase diagram with several stable and metastable forms. Finally, as the synthesis and crystallization procedure must not necessarily produce large crystals, a far greater number of synthesis routes could be investigated, hence allowing in depth studies on how factors in the synthesis determine the crystal structure obtained.

ASSOCIATED CONTENT

Supporting Information

The Supporting Information is available free of charge at https://pubs.acs.org/doi/10.1021/acs.cgd.2c00406.

Crystallographic data; ATR-FTIR spectra; binuclear Co2(TFMBz)4 secondary building units and ladder chains; details of chain packing; void space analysis; SEM micrograph; thermal variation of $1/\chi$; powder X-ray diffractograms; and fit of the rigid-body Rietveld refinement (PDF)

Accession Codes

CCDC 2141822−2141823, 2141825, 2144631, and 2144678 contain the supplementary crystallographic data for this paper. These data can be obtained free of charge via www.ccdc.cam.ac.uk/data_request/cif, or by emailing data_request@ccdc.cam.ac.uk, or by contacting The Cambridge Crystallographic Data Centre, 12 Union Road, Cambridge CB2 1EZ, UK; fax: +44 1223 336033.

AUTHOR INFORMATION

Corresponding Authors

Mauro Gemmi − *Center for Materials Interfaces, Electron Crystallography, Istituto Italiano di Tecnologia, 56025 Pontedera, Italy;* orcid.org/0000-0001-9542-3783; Email: mauro.gemmi@iit.it

José A. Ayllón − *Departamento de Química, Universidad Autónoma de Barcelona, 08193 Bellaterra, Barcelona, Spain;* orcid.org/0000-0001-7965-7424; Email: JoseAntonio.Ayllon@uab.es

Authors

Francesco Papi − *Center for Materials Interfaces, Electron Crystallography, Istituto Italiano di Tecnologia, 56025 Pontedera, Italy*

Albert Rosado − *Instituto de Ciencia de Materiales de Barcelona (ICMAB-CSIC), 08193 Bellaterra, Barcelona, Spain;* orcid.org/0000-0003-3222-9566

Oriol Vallcorba − *ALBA Synchrotron Light Source, 08290 Cerdanyola del Vallés, Barcelona, Spain*

Arianna E. Lanza − *Center for Materials Interfaces, Electron Crystallography, Istituto Italiano di Tecnologia, 56025 Pontedera, Italy;* orcid.org/0000-0002-7820-907X

Núria Portolés-Gil − *Instituto de Ciencia de Materiales de Barcelona (ICMAB-CSIC), 08193 Bellaterra, Barcelona, Spain*

https://doi.org/10.1021/acs.cgd.2c00406
Cryst. Growth Des. 2022, 22, 4463−4471

Ana M. López-Periago − *Instituto de Ciencia de Materiales de Barcelona (ICMAB-CSIC), 08193 Bellaterra, Barcelona, Spain;* orcid.org/0000-0002-3777-3205

Concepción Domingo − *Instituto de Ciencia de Materiales de Barcelona (ICMAB-CSIC), 08193 Bellaterra, Barcelona, Spain;* orcid.org/0000-0002-6976-8283

Complete contact information is available at: https://pubs.acs.org/10.1021/acs.cgd.2c00406

Author Contributions

The manuscript was written through contributions of all authors. All authors have given approval to the final version of the manuscript.

Notes

The authors declare no competing financial interest.

This work was done in the framework of the doctoral program "Chemistry" of the Universitadad Autónoma de Barcelona by A.R. who acknowledge the FPI grant.

■ ACKNOWLEDGMENTS

This work was supported by the Spanish Ministry of Science and Innovation MICINN through the Severo Ochoa Program for Centers of Excellence (CEX2019-000917-S) and the Spanish National Plan of Research with projects PID2020-115631GB-I00. F.P., A.E.L., and M.G. would like to thank Regione Toscana for funding the purchase of the ASI MEDIPIX detector through the FELIX project (POR CREO FERS 2014−2020). The measures for the elucidation of the crystal structure of compound **1** were performed at the XALOC beamline at ALBA Synchrotron with the collaboration of ALBA staff.

■ REFERENCES

(1) Furukawa, H.; Cordova, K. E.; O'Keeffe, M.; Yaghi, O. M. The Chemistry and Applications of Metal-Organic Frameworks. *Science* **2013**, *341*, 1230444.

(2) Silva, P.; Vilela, S. M. F.; Tomé, J. P. C.; Almeida Paz, F. A. Multifunctional metal-organic frameworks: from academia to industrial applications. *Chem. Soc. Rev.* **2015**, *44*, 6774−6803.

(3) Ji, Z.; Wang, H.; Canossa, S.; Wuttke, S.; Yaghi, O. M. Pore Chemistry of Metal−Organic Frameworks. *Adv. Funct. Mater.* **2020**, *30*, 2000238.

(4) Wang, Q.; Astruc, D. State of the Art and Prospects in Metal−Organic Framework (MOF)-Based and MOF-Derived Nanocatalysis. *Chem. Rev.* **2020**, *120*, 1438−1511.

(5) Rojas, S.; Horcajada, P. Metal−Organic Frameworks for the Removal of Emerging Organic Contaminants in Water. *Chem. Rev.* **2020**, *120*, 8378−8415.

(6) Tan, Y. S.; Otero-de-la-Roza, A.; Jotani, M. M.; Tiekink, E. R. T. Snap Frozen! Capturing Two Metastable Polymorphs in a Tetramorphic One-Dimensional Coordination Polymer Constructed from Cadmium, Dithiophosphate, and 4-Pyridinealdazine. *Cryst. Growth Des.* **2020**, *20*, 3272−3283.

(7) Moulton, B.; Zaworotko, M. J. From Molecules to Crystal Engineering: Supramolecular Isomerism and Polymorphism in Network Solids. *Chem. Rev.* **2001**, *101*, 1629−1658.

(8) Hennigar, T. L.; MacQuarrie, D. C.; Losier, P.; Rogers, R. D.; Zaworotko, M. J. Supramolecular Isomerism in Coordination Polymers: Conformational Freedom of Ligands in $[Co(NO_3)_2(1,2\text{-bis}(4\text{-pyridyl})\text{ethane})_{1.5}]_n$. *Angew. Chem., Int. Ed.* **1997**, *36*, 972−973.

(9) Lee, E.; Hongu, H.; Temma, H.; Toya, M.; Ikeda, M.; Kuwahara, S.; Habata, Y. Solvent-Dependent Formations of Supramolecular Isomers and a Single-Crystal to Single-Crystal Transformation from a Cyclic Dimer Complex to a One-Dimensional Coordination Polymer. *Cryst. Growth Des.* **2020**, *20*, 3284−3292.

(10) Gheorghe, A.; Imaz, I.; van der Vlugt, J. I.; Maspoch, D.; Tanase, S. Tuning the supramolecular isomerism of MOF-74 by controlling the synthesis conditions. *Dalton Trans.* **2019**, *48*, 10043−10050.

(11) Karmakar, A.; Paul, A.; Pombeiro, A. J. L. Recent advances on supramolecular isomerism in metal organic frameworks. *CrystEngComm* **2017**, *19*, 4666−4695.

(12) Portolés-Gil, N.; López-Periago, A. M.; Borrás, A.; Fraile, J.; Solano, E.; Vallcorba, O.; Planas, J. G.; Ayllón, J. A.; Domingo, C. Tuning the Structure and Flexibility of Coordination Polymers via Solvent Control of Tritopic Triazine Conformation during Crystallization. *Cryst. Growth Des.* **2020**, *20*, 3304−3315.

(13) Ju, H.; Park, I.-H.; Lee, E.; Kim, S.; Jung, J. H.; Ikeda, M.; Habata, Y.; Lee, S. S. Guest-triggered assembly of zinc(II) supramolecular isomers with accompanying dimensional change and reversible single-crystal-to-single-crystal transformation. *CrystEngComm* **2016**, *18*, 1600−1608.

(14) Zhang, J.-P.; Huang, X.-C.; Chen, X.-M. Supramolecular isomerism in coordination polymers. *Chem. Soc. Rev.* **2009**, *38*, 2385.

(15) Pavlishchuk, A. V.; Kolotilov, S. V.; Zeller, M.; Shvets, O. V.; Fritsky, I. O.; Lofland, S. E.; Addison, A. W.; Hunter, A. D. Magnetic and Sorption Properties of Supramolecular Systems Based on Pentanuclear Copper(II) 12-Metallacrown-4 Complexes and Isomeric Phthalates: Structural Modeling of the Different Stages of Alcohol Sorption. *Eur. J. Inorg. Chem.* **2011**, *2011*, 4826−4836.

(16) Peng, Y.-F.; Ge, H.-Y.; Li, B.-Z.; Li, B.-L.; Zhang, Y. Three Supramolecular Isomers of Square Grid Networks from the Assembly of a Flexible Spacer and $Co(NCS)_2$: Structures and Polymer Transformation. *Cryst. Growth Des.* **2006**, *6*, 994−998.

(17) Wang, S.; Peng, Y.; Wei, X.; Zhang, Q.; Wang, D.; Dou, J.; Li, D.; Bai, J. Temperature-dependent supramolecular isomerism in three zinc coordination polymers with pamoic acid and 1,4-bis(imidazole-1-ylmethyl)-benzene. *CrystEngComm* **2011**, *13*, 5313.

(18) Liu, G.-l.; Song, J.-B.; Qiu, Q.-m.; Li, H. Syntheses, structures, and magnetic properties of three supramolecular isomeric Cu(II) square grid networks: solvents effect on the ligand linkages. *CrystEngComm* **2020**, *22*, 1321−1329.

(19) Masaoka, S.; Tanaka, D.; Nakanishi, Y.; Kitagawa, S. Reaction-Temperature-Dependent Supramolecular Isomerism of Coordination Networks Based on the Organometallic Building Block$[CuI_2(\mu^2\text{-BQ})(\mu^2\text{-OAc})_2]$. *Angew. Chem., Int. Ed.* **2004**, *43*, 2530−2534.

(20) Galet, A.; Muñoz, M. C.; Martínez, V.; Real, J. A. Supramolecular isomerism in spin crossover networks with aurophilic interactions. *Chem. Commun.* **2004**, *20*, 2268−2269.

(21) Ye, Z.-M.; He, C.-T.; Xu, Y.-T.; Krishna, R.; Xie, Y.; Zhou, D.-D.; Zhou, H.-L.; Zhang, J.-P.; Chen, X.-M. A New Isomeric Porous Coordination Framework Showing Single-Crystal to Single-Crystal Structural Transformation and Preferential Adsorption of 1,3-Butadiene from C4 Hydrocarbons. *Cryst. Growth Des.* **2017**, *17*, 2166−2171.

(22) Gao, X.; Fu, A.-Y.; Wang, Y.-Y. Shape-Asymmetry Supramolecular Isomerism in Asymmetrical Ligand PCPs and the Expression Method of Three-Level Isomerism. *Inorg. Chem.* **2016**, *55*, 4330−4334.

(23) Biradha, K.; Sarkar, M.; Rajput, L. Crystal engineering of coordination polymers using 4,4′-bipyridine as a bond between transition metal atoms. *Chem. Commun.* **2006**, 4169−4179.

(24) Shen, J.-B.; Wu, X.-Y.; Chen, X.-J.; Zhao, G.-L. Poly[[μ-aqua-bis-(μ-4,4′-bi-pyridine-κ2N:N′)bis-(μ-3-hy-droxy-adamantane-1-carboxyl-ato-κ2O:O′)bis-(3-hy-droxy-adamantane-1-carboxyl-ato-κO)-dicobalt(II)] hepta-hydrate]. *Acta Crystallogr., Sect. E: Struct. Rep. Online* **2011**, *67*, m558−m559.

(25) Hsu, S.-C.; Chiang, P.-S.; Liu, H.-K.; Lo, S.-H.; Lin, C.-H. Multi-Dimensional Cobalt(II) and Nickel(II) Coordination Polymers. *J. Chin. Chem. Soc.* **2012**, *59*, 18−27.

(26) Wang, X.; Liu, G.; Chen, B.; Bi, Y.; Lin, H. A 3-D metal-organic framework constructed with cobalt(II), 1,3-di(4-pyridyl)propane (bpp) and 3,5-dinitrobenzoate (DNBA) with methyl-3,5-dinitroben-

zoate (MDNBA) by *in-situ* synthesis as a guest. *J. Coord. Chem.* **2008**, *61*, 1635−1644.
(27) Fontanet, M.; Rodríguez, M.; Fontrodona, X.; Romero, I.; Teixidor, F.; Viñas, C.; Aliaga-Alcalde, N. Carving a 1D Co^{II}-carboranylcarboxylate system by using organic solvents to create stable trinuclear molecular analogues: complete structural and magnetic studies. *Dalton Trans.* **2016**, *45*, 10916−10927.
(28) Tomkowicz, Z.; Ostrovsky, S.; Foro, S.; Calvo-Perez, V.; Haase, W. Magnetooptical and Structural Investigations of Five Dimeric Cobalt(II) Complexes Mimicking Metalloenzyme Active Sites. *Inorg. Chem.* **2012**, *51*, 6046−6055.
(29) Karmakar, A.; Sarma, R. J.; Baruah, J. B. Synthesis and characterisation of dinuclear and mononuclear Cobalt (II) benzoate complexes. *Polyhedron* **2007**, *26*, 1347−1355.
(30) Burley, J. C.; Prior, T. J. m_2-Aqua-bis-(m_2-trifluoro-aceto-k^2-O,O')bis-[bis-(pyridine- kN)(trifluoro-acetato kO)cobalt(II)]. *Acta Crystallogr., Sect. E: Struct. Rep. Online* **2005**, *61*, m1422−m1424.
(31) Ma, D.-Y.; Guo, H.-F.; Lu, K.; Pan, Y.; Qin, L.; Blatov, V. A. A 1D → 3D Two-Fold Interpenetration Array Formed by Hydrogen-Bonding Interactions. *Z. Anorg. Allg. Chem.* **2012**, *638*, 992−995.
(32) Song, Y. J.; Kwak, H.; Lee, Y. M.; Kim, S. H.; Lee, S. H.; Park, B. K.; Jun, J. Y.; Yu, S. M.; Kim, C.; Kim, S.-J.; Kim, Y. Metal-directed supramolecular assembly of metal(II) benzoates (M=Co, Ni, Cu, Zn, Mn, and Cd) with 4,4′-bipyridine: Effects of metal coordination modes and novel catalytic activities. *Polyhedron* **2009**, *28*, 1241−1252.
(33) Lu, J.; Yu, C.; Niu, T.; Paliwala, T.; Crisci, G.; Somosa, F.; Jacobson, A. J. One-Dimensional Coordination Polymers of Cobalt with 4,4'-Bipyridine: Syntheses and Structures. *Inorg. Chem.* **1998**, *37*, 4637−4640.
(34) Perec, M.; Baggio, R. Di-μ-acetato-bis[(acetato-κ 2 O,O′)bis-(isonicotinamide-κ N)copper(II)]. *Acta Crystallogr., Sect. E: Struct. Rep. Online* **2010**, *66*, m275−m276.
(35) Peña-Rodríguez, R.; Rivera, J. M.; Colorado-Peralta, R.; Duarte-Hernández, A. M.; Flores-Parra, A. Bis(μ 2 -benzoato-κ 2 O : O′)bis[(benzoato-κ 2 O , O ′)bis(4,4′-bipyridine-κ N)cobalt(II)]−benzoic acid (1/6). *Acta Crystallogr., Sect. E: Struct. Rep. Online* **2014**, *70*, m21−m22.
(36) Dojer, B.; Pevec, A.; Belaj, F.; Jagličić, Z.; Kristl, M.; Drofenik, M. Structural and magnetic properties of cobalt(II) complexes with pyridinecarboxamide ligands. *J. Mol. Struct.* **2014**, *1076*, 713−718.
(37) Sun, Y.; Wang, Z.; Zhang, H.; Cao, Y.; Zhang, S.; Chen, Y.; Huang, C.; Yu, X. Self-assembly of three novel mixed-ligand coordination polymers: Formation of 2-D grids, 1-D chains and ladders and crystal band structure. *Inorg. Chim. Acta* **2007**, *360*, 2565−2572.
(38) Zheng, Y.-Z.; Tong, M.-L.; Chen, X.-M. Syntheses, structures and magnetic properties of five coordination polymers derived via in situ metal−ligand reactions of 2-phenyl-malonic acid. *J. Mol. Struct.* **2006**, *796*, 9−17.
(39) Zhuang, W.; Zheng, X.; Li, L.; Liao, D.; Ma, H.; Jin, L. Structural diversity and properties of M(ii) 4-carboxyl phenoxyacetate complexes with 0D-, 1D-, 2D- and 3D M-cpoa framework. *CrystEngComm* **2007**, *9*, 653−667.
(40) Brog, J.-P.; Chanez, C.-L.; Crochet, A.; Fromm, K. M. Polymorphism, what it is and how to identify it: a systematic review. *RSC Adv.* **2013**, *3*, 16905−16931.
(41) Wriedt, M.; Jeß, I.; Näther, C. Synthesis, Crystal Structures, and Thermal Properties of New [ZnX 2 (2,5-dimethylpyrazine)] (X = Cl, Br, I) Coordination Compounds. *Eur. J. Inorg. Chem.* **2009**, *2009*, 363−372.
(42) Sun, J.-K.; Jin, X.-H.; Chen, C.; Zhang, J. Thermally Triggered Reversible Transformation between Parallel Staggered Stacking and Plywood-Like Stacking of 1D Coordination Polymer Chains. *Inorg. Chem.* **2010**, *49*, 7046−7051.
(43) Jia, H.-P.; Li, W.; Ju, Z.-F.; Zhang, J. A two-step field-induced magnetic transition in spin-canted systems observed only for the Co II coordination polymer. *Chem. Commun.* **2008**, *3*, 371−373.
(44) Cui, P.; Wu, J.; Zhao, X.; Sun, D.; Zhang, L.; Guo, J.; Sun, D. Two Solvent-Dependent Zinc(II) Supramolecular Isomers: Rare kgd and Lonsdaleite Network Topologies Based on a Tripodal Flexible Ligand. *Cryst. Growth Des.* **2011**, *11*, 5182−5187.
(45) Song, J.-F.; Luo, J.-J.; Jia, Y.-Y.; Xin, L.-D.; Lin, Z.-Z.; Zhou, R.-S. Solvent-induced construction of two zinc supramolecular isomers: synthesis, framework flexibility, sensing properties, and adsorption of dye molecules. *RSC Adv.* **2017**, *7*, 36575−36584.
(46) Biswas, S.; Gómez-García, C. J.; Clemente-Juan, J. M.; Benmansour, S.; Ghosh, A. Supramolecular 2D/3D Isomerism in a Compound Containing Heterometallic CuII2CoII Nodes and Dicyanamide Bridges. *Inorg. Chem.* **2014**, *53*, 2441−2449.
(47) Jia, Y.; Li, H.; Guo, Q.; Zhao, B.; Zhao, Y.; Hou, H.; Fan, Y. Template-Induced Structural Isomerism of Pyridine-2,3-dicarboxylate and Pb^{II} with Similar High Stability and Different Fluorescent Properties. *Eur. J. Inorg. Chem.* **2012**, *2012*, 3047−3053.
(48) Wu, J.-Y.; Hsiao, C.-C.; Chiang, M.-H. Concomitant Crystallization of Genuine Supramolecular Isomeric Rhombus Grid and Ribbon. *Cryst. Growth Des.* **2014**, *14*, 4321−4328.
(49) Coudert, F.-X.; Evans, J. D. Nanoscale metamaterials: Meta-MOFs and framework materials with anomalous behavior. *Coord. Chem. Rev.* **2019**, *388*, 48−62.
(50) Park, J.; Howe, J. D.; Sholl, D. S. How Reproducible Are Isotherm Measurements in Metal−Organic Frameworks? *Chem. Mater.* **2017**, *29*, 10487−10495.
(51) Wang, C.; Zhou, D.-D.; Gan, Y.-W.; Zhang, X.-W.; Ye, Z.-M.; Zhang, J.-P. A partially fluorinated ligand for two super-hydrophobic porous coordination polymers with classic structures and increased porosities. *Natl. Sci. Rev.* **2021**, *8*, nwaa094.
(52) Holden, D.; Chong, S. Y.; Chen, L.; Jelfs, K. E.; Hasell, T.; Cooper, A. I. Understanding static, dynamic and cooperative porosity in molecular materials. *Chem. Sci.* **2016**, *7*, 4875−4879.
(53) Jing, X.-H.; Yi, X.-C.; Gao, E.-Q.; Blatov, V. A. Synthesis, structure, topology and magnetic properties of cobalt(II) coordination polymers with 2-nitrobiphenyl-4,4′-dicarboxylic acid and bis-(pyridyl) ligands. *Dalton Trans.* **2012**, *41*, 14316−14328.
(54) Kim, J.; Jo, H.; Yoon, S. W.; Lee, M. H.; Choi, W. J.; Choi, K. Y.; Ok, K. M. Synthesis, Structure, and Characterization of Variable Chains in a Series of Transition Metal Coordination Compounds. *Eur. J. Inorg. Chem.* **2020**, *2020*, 452−460.
(55) Karmakar, A.; Sarma, R. J.; Baruah, J. B. Polymorphism in an Aqua-Bridged, Dinuclear 2-Nitrobenzoate Complex of Cobalt(II). *Eur. J. Inorg. Chem.* **2007**, *2007*, 643−647.

NOTE ADDED AFTER ASAP PUBLICATION

Published ASAP June 2, 2022; Name of third author corrected June 14, 2022.

https://doi.org/10.1021/acs.cgd.2c00406
Cryst. Growth Des. 2022, 22, 4463−4471